^{1}H and ^{13}C NMR study of tetrahydro-1,4-benzothiazepine conformations †

Alan R. Katritzky,*[a] Novruz G. Akhmedov,[a] Ion Ghiviriga[b] and Peter J. Steel[c]

[a] *Center for Heterocyclic Compounds, Department of Chemistry, University of Florida, P.O. Box 117200, Gainesville, FL 32611-7200, USA. E-mail: katritzky@chem.ufl.edu; Fax: (352) 392-9199*
[b] *Department of Chemistry, University of Florida, P.O. Box 117200, Gainesville, FL 32611-7200, USA*
[c] *Department of Chemistry, University of Canterbury, Christchurch, New Zealand*

Received (in Cambridge, UK) 13th June 2002, Accepted 13th August 2002
First published as an Advance Article on the web 3rd October 2002

The variable temperature (298–178 K) ^{1}H NMR spectra of tetrahydro-1,4-benzothiazepines **1**–**10** are described and discussed. Compounds **2**–**10** exist as two puckered mirror-image (enantiomorphic) conformers, with benzothiazepine ring chair-to-chair interconversion barriers of *ca.* 10 kcal mol^{-1} in CD_2Cl_2 solution. A similar interconversion was detected for compound **1**, of lower symmetry. The ground state conformations of **1**–**10** were assigned on the basis of the magnitudes of ^{1}H–^{1}H vicinal coupling constants. The ^{1}H and ^{13}C NMR spectral assignments were determined by ^{1}H–^{1}H COSY, HETCOR, and NOESY experiments. The stereochemistry and conformation of compound **1** was further confirmed by a single crystal X-ray structure determination.

Introduction

1,4-Benzothiazepine derivatives are of considerable interest from both the synthetic,[1a–f] and pharmacological view points.[2a–c]

A search of the 2001 version of the Cambridge Crystallographic Database for 2,3,4,5-tetrahydro-1,4-benzothiazepines located a 2-phenylbenzothiazepin-5-one as the only entry;[3a] the nearest heteroanalogue was 7-acetyl-2,3,4,5-tetrahydro-5*H*-1,4-benzoxazepine.[3b] Despite the enormous chemical and pharmacological interest in compounds bearing substituents at positions 2, 3, and/or 5 in the 1,4-benzothiazepine ring, there have been few studies concerning their conformational behaviour.[1a,1c] The conformations of 2,3,4,5-tetrahydro-1,4-benzothiazepines bearing a substituent on nitrogen in the seven membered ring have not previously been discussed. In a continuation of our previous synthetic study,[4] we now report a ^{1}H and ^{13}C NMR conformational investigation of ten *N*-substituted 2,3,4,5-tetrahydro-1,4-benzothiazepines.

The conformations of seven membered ring heterocycles having two heteroatoms in positions 1,3-(*O*,*O*); 1,5-(*O*, *O*); 2,4-(*O*, *O*),[5a–c] 2,4-(*S*, *S*),[5d] 1,5-(*S*, *S*),[5d,e] 1,5-(*S*, *N*),[5f–h] 1,4-(*N*,*N*)[5i] and 1,5-(*N*,*N*)[5h] have been studied extensively. Such compounds show conformational behaviour significantly different from analogues containing a single heteroatom.[5a,5c,5j,5k] The additional heteroatom influences the conformational equilibria, mainly by electrostatic interactions and intramolecular H-bonding.[6] In the above mentioned literature data, it was also established that conformational properties of mono-heteroanalogues of benzocycloheptene depend on the position of the heteroatom and also on the polarity of the substituents in the seven membered ring. Di-heteroanalogues of benzocycloheptene showed three seven-membered ring geometries: the chair (C), boat (B) and twist-boat (TB) conformations, as derivatives of benzocycloheptene[7] (Scheme 1).

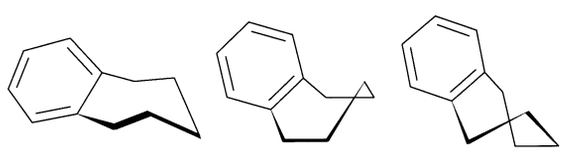

Scheme 1

In the present work we report a conformational study of *N*-substituted 1,4-benzothiazepines **1**–**10** (Scheme 2). The

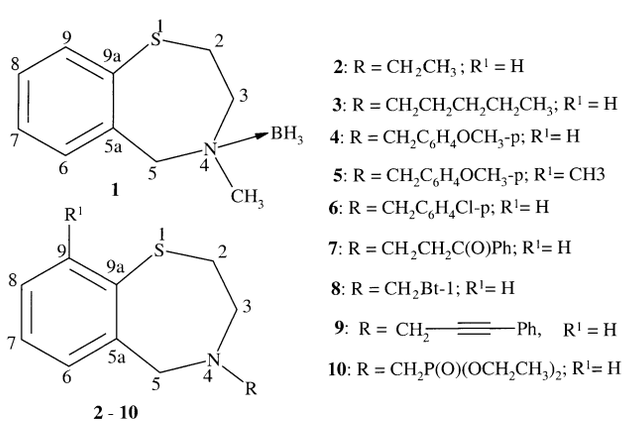

Scheme 2

energy barriers ($\Delta G^{\#}$, kcal mol^{-1}) for the conformational inversion of tetrahydro-1,4-benzothiazepines (**2**–**10**) were determined in CD_2Cl_2 solution. It was established that *N*-substituted 1,4-benzothiazepines **2**–**10** display only two enantiomorphic chair conformations, which exchange through a ring inversion (Scheme 3), in the same manner as benzocycloheptene itself.[7]

† Electronic supplementary information (ESI) available: crystal data, structure refinement and a perspective view of the X-ray crystal structure of **1**. See http://www.rsc.org/suppdata/p2/b2/b205768a/

 DOI: 10.1039/b205768a

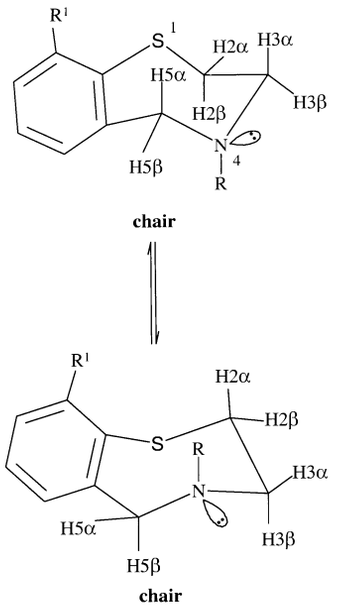

Scheme 3

Results and discussion

The assignments of the proton spectra for compounds of **1**–**10** (Scheme 2) are based on the ^{1}H–^{1}H COSY, NOE difference and NOESY experiments. The spectral data for **1**–**10** are reported in Table 1.

Assignment of the ^{1}H NMR spectra of compounds 1–10 and conformations of the seven-membered rings

Room temperature spectra. In the ^{1}H NMR spectra of **2**–**10**, the singlet signals in the region 4.09–4.26 ppm (see Table 1) can easily be assigned to H-5 due to the deshielding effect of the electronegative nitrogen atom. In a similar manner, the multiplet signals (AA′XX′ type spectra) in regions 3.21–3.45 and 2.71–2.87 ppm belong to H-3 and H-2, respectively.

Proton–proton connectivities, deduced from selective irradiation or COSY experiments, allowed the assignment of all the *N*-substituent proton signals (see Table 1). At room temperature, the averaging of C-5 proton signals indicates the presence of two mirror images, puckered configurational isomers, which rapidly interconvert on the NMR time scale. This fast exchange renders equivalent the protons on either α or β faces for positions 2, 3, and 5. For all compounds **1**–**10**, proton signals of H-6 of the fused benzene ring were upfield in comparison to H-9 (see Table 1). The proton H-6 was assigned from the NOE difference effect that was observed when the H-5 proton signal of the seven membered ring was irradiated.

For compound **1**, containing the $N(CH_3)BH_3$ fragment, the protons on the α and β faces are non-equivalent. The assignment of the doublet at 4.11 ppm (H5eq) of **1** is supported by the mutual NOE difference experiments. The H5 doublet at 4.11 ppm displayed a larger NOE with H-6 at 7.25 ppm, therefore the doublet at 4.11 ppm was assigned to the equatorial position (H5eq). The proton spectrum of **1** (Fig. 1) at −93 °C displays sharp lines of H5ax at 4.50 ppm. However, at temperatures between 50 °C and −20 °C the peak H-5ax broadened but became sharp again at temperatures around −93 °C. Similarly, the proton (H5eq, 4.11ppm) broadened at room temperature but sharpened again at low temperature (−93 °C). These features can be explained as follows: at low temperatures only one conformer is present in appreciable concentration but as the temperature increases, a second minor conformer also exists in equilibrium with the first and the rate of conformational exchange is comparable to the frequency separation of the isochronous sites. However, at higher temperatures, the conformational equilibrium is fast on the NMR time-scale, and the averaged spectrum has narrow lines.

Compound **1** is observed to exist predominantly in the chair conformation, having the BH_3 group in the equatorial position and the methyl group in the axial position. The BH_3 preference for the equatorial position in **1** is deduced from the ^{1}H, ^{13}C and

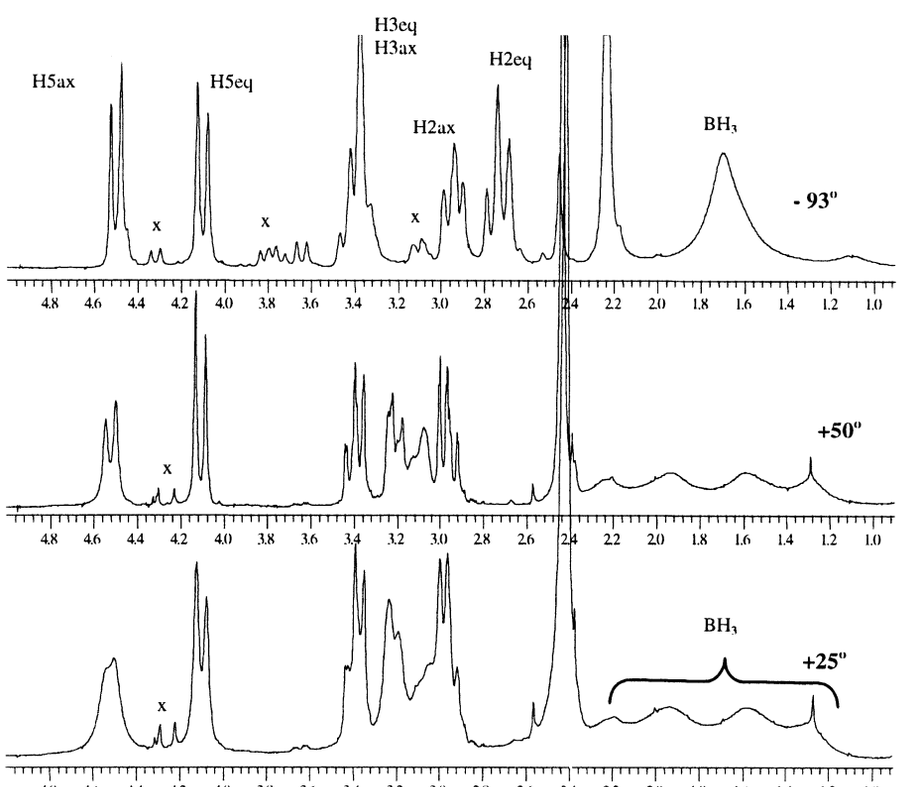

Fig. 1 Aliphatic portion of temperature dependent ^{1}H NMR spectra of **1** in CD_2Cl_2 (x denotes an impurity).

Table 1 The ^{1}H NMR chemical shifts (δ/ppm), multiplicity, and coupling constants (J/Hz) of seven-membered ring and alkyl chain (H-4′) protons for compounds **1**–**10**[a] in CD_2Cl_2

Comp	T/°C	H-2	H-3	H-5	H-4′
1[b]	+25	2.92–3.12 (m)	3.31–3.43 (m)	4.52 (br d, H5ax) 4.11 (d, H5eq)	2.42 (s)
	−93	2.94 (t, H2ax) 2.72 (d, H2eq) J_{AB} = 15.2 $^3J_{H2ax,\ H3ax}$ = 11.8	3.21 (br d) J_{AB} = 14.4 3.32–3.42 (m) H3ax + H3eq	J_{AB} = 14.1 4.50 (d, H5ax) 4.11 (d, H5eq) J_{AB} = 14.2	2.24 (s)
2[c]	+25	2.73–2.77 (m)	3.28–3.31 (m)	4.11 (s)	2.44 (quartet)
	−93	2.89 (t, H2ax) 2.40 (d, H2eq) J_{AB} = 14.2 $^3J_{H2ax,\ H3ax}$ = 11.5	3.18 (t, H3ax) 3.39 (d, H3eq) J_{AB} = 13.9 $^3J_{H3ax,\ H2ax}$ = 11.5	4.25 (d, H5ax) 3.94 (d, H5eq) J_{AB} = 14.1	2.31 (dq, A part of H-4′) 2.19 (dq, B part of H-4′) J_{AB} = 12.2 $^3J_{H\text{-}4,\ CH3}$ = 6.9
3[d]	+25	2.72–2.75 (m)	3.27–3.30 (m)	4.09 (s)	2.31–2.36 (m)
	−92	2.91 (t, H2ax) 2.40 (d, H2eq) J_{AB} = 14.5 $^3J_{H2ax,\ H3ax}$ = 11.8	3.18 (t, H3ax) 3.38 (d, H3eq) J_{AB} = 13.8 $^3J_{H3ax,\ H2ax}$ = 11.8	4.25 (d, H5ax) 3.91 (d, H5eq) J_{AB} = 14.4	2.25 (dq, A part of H-4′) 2.11 (dq, B part of H-4′) J_{AB} = 12.2 $^3J_{H\text{-}4',\ CH3}$ = 6.9
4[e]	+25	2.76–2.79 (m)	3.26–3.29 (m)	4.09 (s)	3.48 (s)
	−90	2.98 (t, H-2ax) 2.45 (d, H-2eq) J_{AB} = 14.5 $^3J_{H2ax,\ H3ax}$ = 11.6	3.16 (t, H-3ax) 3.28 (d, H-3eq) J_{AB} = 13.6 $^3J_{H3ax,\ H2ax}$ = 11.6	4.28 (d, H5ax) 3.85 (d, H5eq) J_{AB} = 14.4	3.46 (d, A part of H-4′) 3.29 (d, B part of H-4′) J_{AB} = 13.6
5[f]	+25	2.76–2.80 (m)	3.21–3.24 (m)	4.09 (s)	3.52 (s)
	−92	2.87 (t, H2ax) 2.52 (d, H2eq) J_{AB} = 14.3 $^3J_{H2ax,\ H3ax}$ = 11.4	3.12 (t, H3ax) 3.27 (d, H3eq) J_{AB} = 14.8 $^3J_{H3ax,\ H2ax}$ = 11.4	4.30 (d, H5ax) 3.87 (d, H5eq) J_{AB} = 14.3	3.52 (d, A part of H-4′) 3.28 (d, B part of H-4′) J_{AB} = 12.6
6[g]	+25	2.77–2.81 (m)	3.29–3.33 (m)	4.09 (s)	3.53 (s)
	−93	2.95 (t, H2ax) 2.46 (d, H2eq) J_{AB} = 14.5 $^3J_{H2ax,\ H3ax}$ = 11.8	3.22 (t, H3ax) 3.32 (d, H3eq) J_{AB} = 14.3 $^3J_{H3ax,\ H2ax}$ = 11.8	4.26 (d, H5ax) 3.78 (d, H5eq) J_{AB} = 14.4	3.46 (d, A part of H-4′) 3.33 (d, B part of H-4′) J_{AB} = 13.1
7[h]	+25	2.76–2.79 (m)	3.32–3.35 (m)	4.17 (s)	3.23 (nonresolved)
	−93	3.00 (t, H2ax) 2.47 (d, H2eq) J_{AB} = 14.3 $^3J_{H2ax,\ H3ax}$ = 11.4	3.27 (nonresolved) 3.46 (d, H3eq) J_{AB} = 12.8	4.37 (d, H5ax) 4.00 (d, H5eq) J_{AB} = 14.6	
8[i]	+25	2.84–2.87 (m)	3.39–3.42 (m)	4.20 (s)	5.42 (s)
	−93	2.89 (t, H2ax) 2.70 (d, H2eq) J_{AB} = 14.8 $^3J_{H2ax,\ H3ax}$ = 11.8	3.10 (t, H3ax) 3.54 (d, H3eq) J_{AB} = 14.1 $^3J_{H3ax,\ H2ax}$ = 11.8	4.14 (d, H5ax) 4.02 (d, H5eq) J_{AB} = 14.5	5.54 (d, A part of H-4′) 5.27 (d, B part of H-4′) J_{AB} = 13.8
9[j]	+25	2.82–2.85 (m)	3.38–3.41 (m)	4.21 (s)	3.44 (br s)
	−93	2.88 (t, H2ax) 2.61 (d, H2eq) J_{AB} = 14.4 $^3J_{H2ax,\ H3ax}$ = 11.5	3.25 (t, H3ax) 3.46 (d, H3eq) J_{AB} = 14.8 $^3J_{H3ax,\ H2ax}$ = 11.5	4.28 (d, H5ax) 4.06 (d, H5eq) J_{AB} = 14.5	(nonresolved)
10[k]	+25	2.71–2.74 (m)	3.41–3.45 (m)	4.26 (s)	2.72 (d)
	−93	2.43–2.87 (H-2 + H-4′) (nonresolved)	3.33 (t, H3ax) 3.50 (d, H3eq) J_{AB} = 14.5 $^3J_{H3ax,\ H2ax}$ = 11.3	4.35 (d, H5ax) 4.06 (d, H5eq) J_{AB} = 14.7	$^2J_{H\text{-}4',31P}$ = 10.8 2.43–2.87 (H-4′ + H-2) (nonresolved)

[a] Additional signals: [b] 1.73 (3H, br q, J 94, BH_3) at 25 °C, 1.70 (3H, br s, BH_3) at −93 °C; aromatic protons: 7.48–7.54 (1H, m, H-9), 7.26–7.31 (3H, m, H-6 + H-7 +H-8) .[c] 1.08 (3H, t, J 7.1, CH_3) at 25 °C, 0.98 (3H, t, J 7.1, CH_3) at −93 °C, aromatic protons: 7.25 (1H, dd, J 7.0 and 1.7, H-6), 7.13–7.24 (2H, m, H-7 + H-8), 7.53 (1H, dd, J 6.9 and 1.8, H-9). [d] 0.89 (3H, s, J 7.0, CH_3), 1.18–1.38 (4H, m, 2/H-6′ + 2/H-7′), 1.48 (2H, quintet, J 7.3, H-5′) at 25 °C, 0.79 (3H, s, J 7.0, CH_3), 1.07 (2H, m, 2/H-7′), 1.19 (2H, sextet, J 7.1, 2/H-6′), 1.38 (2H, br quintet, J 7.3, 2/H-5′) at −93 °C, aromatic protons: 7.12–7.22 (2H, m, H-7 + H-8), 7.24 (1H, dd, J 7.2 and 1.8, H-6), 7.52 (1H, dd, J 7.1 and 1.7, H-9) .[e] 3.79 (3H, s, OCH_3), 7.00–7.03 (1H, m, H-6), 7.16–7.19 (2H, m, H-7 + H-8), 7.54–7.57 (1H, m, H-9), 6.87 (2H, d, J 8.7, *m*-Ph), 7.20 (2H, d, J 8.7, *o*-Ph) at 25 °C, 3.75 (3H, s, OCH_3) at −90 °C. [f] 2.49 (3H, s, 9-CH_3), 3.81 (3H, s, OCH_3), 6.87 (3H, m, *m*-Ph + H-6), 7.23 (2H, d, J 8.7, *o*-Ph), 7.12 (1H, ddd, J 7.6, 1.7 and 0.7, H-8), 7.05 (1H, t, J 7.4, H-7) at 25 °C, 2.42 (3H, s, 9-CH_3), 3.76 (3H, s, OCH_3) at −92 °C. [g] 6.96–7.03 (1H, m, H-6), 7.54–7.60 (1H, m, H-9); 7.15–7.21 (2H, m, H-7 + H-8), 7.26 (2H, d, J 8.7, *o*-Ph), 7.32 (2H, d, J 8.7, *m*-Ph) .[h] 2.84 (2H, t, J 7.3, H-5′), 7.14–7.24 (2H, m, H-7 + H-8), 7.28 (1H, dd, J 7.1 and 1.8, H-6), 7.54 (1H, dd, J 7.1 and 1.8, H-9), 7.45–7.51 (2H, m, *meta*/Ph), 7.58–7.61 (1H, m, *p*-Ph), 7.93–7.96 (2H, m, *o*-Ph) at 25 °C, 3.23 (2H, br s, 2/H-4′, not resolv.), 2.67 (2H, br s, 2/H-5′, not resolv.) at −93 °C. [i] 7.56 (1H, dd, J 7.7 and 1.8, H-9), 7.17–7.28 (3H, m, H-6 + H-7 + H-8), 7.40 (1H, ddd, J 8.3, 6.9 and 0.9, Bt-1), 7.52 (1H, ddd, J 8.3, 6.9 and 0.9, Bt-1), 7.68 (1H, dt, J 8.3 and 0.9, Bt-1), 8.05 (1H, dt, J 8.3 and 0.9, Bt-1). [j] 7.15–7.25 (2H, m, H-7 + H-8), 7.31–7.35 (3H, m, *m*-Ph + *p*-Ph + H-6), 7.42–7.46 (2H, m, *o*-Ph); 7.53 (1H, dd, J 7.2 and 1.7, H-9) [k] 4.06–4.16 (4H, m, 2/OCH_2), 1.31 (6H, t, J 7.2, 2/CH_3), 7.14–7.25 (2H, m, H-7 + H-8), 7.33 (1H, dd, J 7.2 and 1.7, H-6), 7.54 (1H, dd, J 7.2 and 1.7, H-9).

^{11}B NMR chemical shifts, as explained below. The application of ^{1}H, ^{13}C and ^{11}B NMR chemical shifts has been previously used for the identification of the preferred conformation of six-membered heterocycles containing the NCH_3–BH_3 structural fragment.[8a–c]

The axial (CH_3) or equatorial (BH_3) preference in **1** was supported by NOESY experiments. The NOE of CH_3 with H2ax indicates that compound **1** adopts a chair conformation in which the CH_3 is axial. These conclusions were confirmed by an X-ray crystal structure determination of **1**. Fig. 2 shows a perspective view of the molecule, which crystallizes in the triclinic space group P-1. The X-ray structure of **1** demonstrates a similar conformation in the solid state. Comparison with related structures in the Cambridge Crystallographic Database

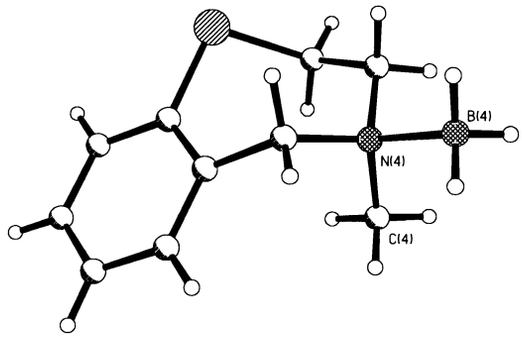

Fig. 2 Perspective view of the X-ray crystal structure of **1**.

showed that the B–N bond length (1.649(2) Å) in **1** is unusually long.[9]

Low temperature spectra. The ^{1}H–^{1}H COSY experiment at low temperature revealed the vicinal and geminal couplings of the protons in positions 2–5, and the geminal couplings were identified in the ^{1}H–^{13}C HETCOR spectrum, yielding a sequence of two methylene groups. The most deshielded methylene CH_2 was assigned to C-5 in the seven membered ring. The axial protons in positions 2 and 3 were identified by two large couplings (*ca.* 10–15 Hz), one geminal and one axial–axial. The ^{1}H chemical shifts and coupling constants of compounds **1**–**10** are given in Table 1.

In contrast to cyclohexane,[10] for which the axial protons appear at high field, the axial protons of the parent benzocycloheptene ring system appear at lower field.[7] The irregular relationship $\delta_{H5ax} > \delta_{H5eq}$ [11] is due to the anisotropy of one of the lone pairs on the sulfur atom to H5ax. At low temperatures, in the ^{1}H NMR spectra of **2**–**10**, each signal of the seven member ring (H-2, H-3, H-5) and side chain H-4′ broadens to give AB type spectra due to the existence of a single chair (C) conformation in which the individual methylene protons (H-2, H-3, H-5 and H-4′) have different environments. As room temperature is approached, the rate of conformational interchange between the two protons of each methylene group of the benzazepine ring increases, resulting in conformationally averaged spectra. The low temperature ^{1}H NMR spectra of **2**–**10** show the same dynamic process with a different rate constant (k, s^{-1}) for ring inversion (see Table 3).

As representative examples of this series of compounds **2**–**10**, variable temperature dependent ^{1}H NMR spectra for compounds **3** (Fig. 3) and **6** (Fig. 4) are shown.

Determination of the thermodynamic parameters (T_c, k_c, $\Delta G^{\#}$) for the conformational ring inversion for compounds 2–10

Using the Eyring equation,[12] the free energy of activation $\Delta G^{\#}$ (Table 2) for the chair-to-chair conformational inversion for compounds **2**–**10** was estimated from the observed coalescence temperature (T_c).

Tetrahydrobenzothiazepines **2**–**10**, as di-heteroanalogues of benzocycloheptene, exhibit higher energy barriers, by *ca.* 2 kcal mol^{-1}, for conformational ring inversion as compared to that of substituted cycloheptanes ($\Delta G^{\#}$ = 7.8 kcal mol^{-1}),[13,14] because the pseudorotation in **2**–**10** is blocked by the presence of the double bond of the fused benzene ring, and ring inversion is considerably slower.

On comparing the values of free energy of activation of benzocycloheptene (10–11 kcal mol^{-1}) [15] with *N*-substituent-2-benzothiazepines **2**–**10**, it was observed that the introduction of a heteroatom (nitrogen) to the benzocycloheptene ring did not significantly change the magnitude of the barrier.

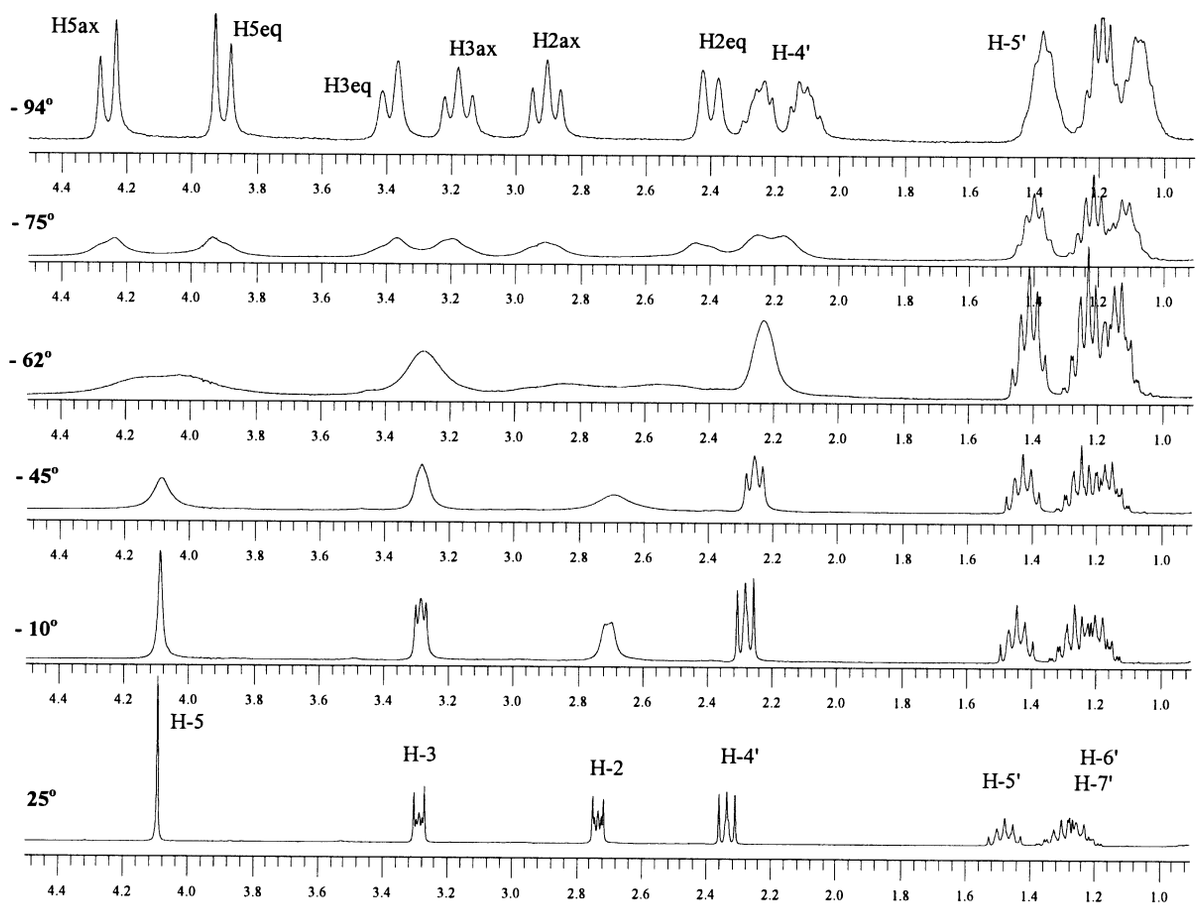

Fig. 3 ^{1}H NMR variable temperature spectra of **3** in CD_2Cl_2.

Table 2 Coalescence temperatures (T_c/°C), methylene shift positions (δ/ppm), geminal coupling constant (J/Hz), rate constant of inversion (k_c/s^{-1} [b]) and free energies of activation ($\Delta G^{\#}$, kcal mol^{-1} [a]) for the conformational inversion of *N*-substitued-1,4-benzothiazepines (**2**–**10**) in CD_2Cl_2

Compound	Proton	δ_A	δ_B	$\delta\nu$/Hz	$^2J_{AB}$/Hz	T_c/°C	k_c/s^{-1}	$\Delta G^{\#}$/kcal mol^{-1}
2	H-2	2.89	2.40	147	14.2	−67	335.4	9.5
	H-5	4.25	3.94	93	14.1	−67	110.8	9.7
3	Proton	—	—	—	—	—	—	—
	H-2	2.91	2.40	153	14.5	−57	348.7	10.0
	H-5	4.25	3.91	102	14.4	−61	239.6	10.0
4	Proton	—	—	—	—	—	—	—
	H-2	2.98	2.45	159	14.5	−52	361.7	10.2
	H-3	3.28	3.16	36	14.5	−61	112.3	10.4
	H-5	4.28	3.85	129	14.4	−53	296.9	10.3
	H-4′	3.46	3.29	51	13.6	−60	135.2	10.3
5	Proton	—	—	—	—	—	—	—
	H-2	2.87	2.52	105	14.3	−41	245.7	11.0
	H-5	4.30	3.87	129	14.3	−39	296.7	10.9
6	Proton	—	—	—	—	—	—	—
	H-2	2.95	2.46	147	14.5	−51	335.7	10.3
	H-5	4.26	3.78	144	14.4	−51	329.1	10.3
7	Proton	—	—	—	—	—	—	—
	H-2	3.00	2.47	159	14.3	−48	361.4	10.4
	H-3	3.46	3.27	57	12.8	−58	144.4	10.5
	H-5	4.37	4.00	111	14.6	−54	258.9	10.3
8	Proton	—	—	—	—	—	—	—
	H-2	2.89	2.70	57	14.8	−63	150.0	10.1
	H-3	3.54	3.10	132	14.1	−59	302.9	10.2
	H-5	4.14	4.02	36	14.5	−65	112.3	10.2
	H-4′	5.54	5.27	81	13.8	−63	194.9	10.0
9	Proton	—	—	—	—	—	—	—
	H-2	2.88	2.61	81	14.4	−63	196.1	10.0
	H-3	3.46	3.25	63	14.8	−63	161.3	10.1
	H-5	4.28	4.06	66	14.5	−62	166.4	10.1
10	Proton	—	—	—	—	—	—	—
	H-3	3.50	3.33	51	14.5	−54	138.0	10.6
	H-5	4.35	4.06	87	14.7	−51	209.0	10.5

[a] $\Delta G^{\#} = 19.14\ T_C\ (9.97 + \log T_C/\delta\nu)$ J mol^{-1} (1cal = 4.18 J) [b] $k_{coalescence} = \pi\ (\Delta\nu^2 + 6J_{AB}^2)^{1/2}/(2^{1/2})$

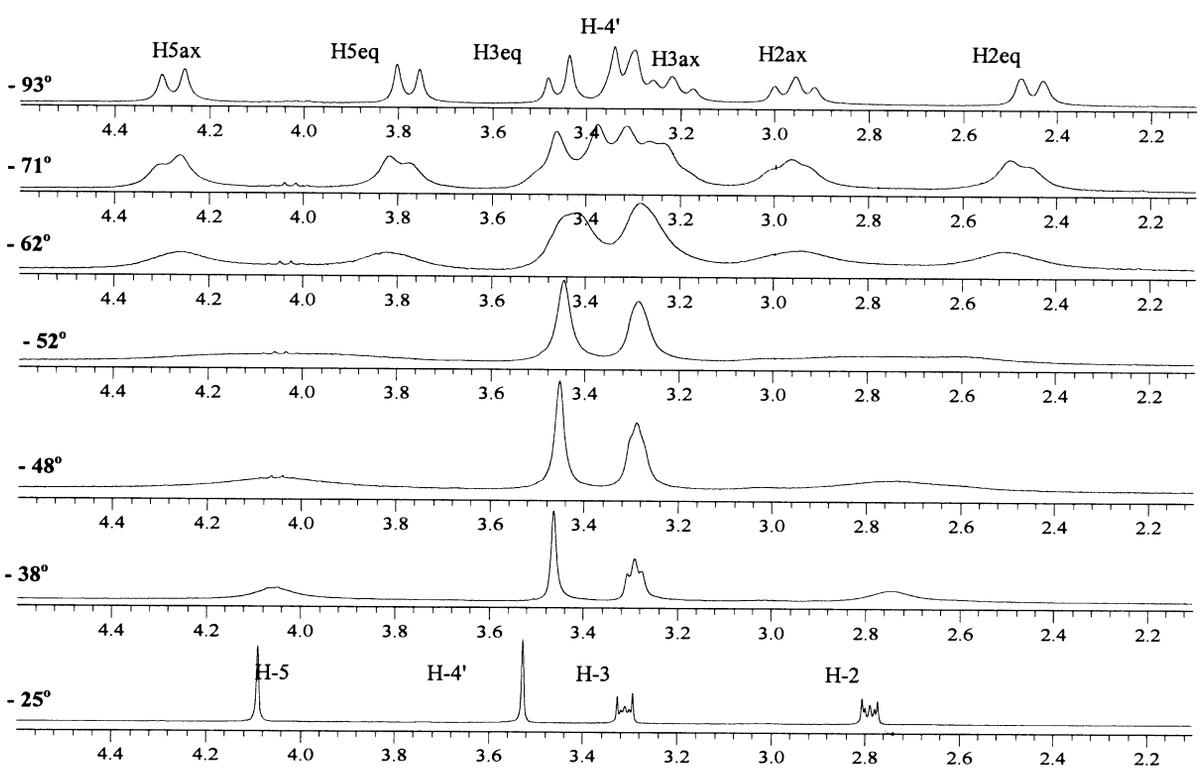

Fig. 4 ^{1}H NMR variable temperature spectra of **6** in CD_2Cl_2 (aliphatic region).

The rate of inversion at the coalescence temperature was calculated from the expression $k_{coalescence} = \pi\ (\Delta\nu^2 + 6J_{AB}^2)^{1/2}/(2^{1/2})$, where $\Delta\nu = \nu_A - \nu_B$ (in Hz) is the difference in chemical shift between the centers of the two doublets arising from the methylene protons, and J is the coupling constant.[15] The rate constants (k, s^{-1}) of inversion of benzothiazepines ring at the corresponding coalescence temperature (T_c) are given in Table 2.

Table 3 ^{13}C NMR spectral data of *N*-substituted-2-benzothiazepines[a] **1**–**10** in CD_2Cl_2

Comp	*T*/°C	C-2	C-3	C-5	C-4′	C-5a	C-6	C-7	C-8	C-9	C-9a
1[b]	25	28.6	63.8	65.9	46.4	136.4	132.7	129.8	128.4	133.3	137.6
	−93	28.3	64.4	65.2	44.1	136.3	132.1	128.7	127.9	132.7	132.1
2[c]	25	30.8	58.3	59.6	47.0	137.6	131.0	127.7	127.6	132.6	143.7
	−93	28.2	57.3	57.8	44.0	136.2	130.5	126.9	126.8	131.8	142.6
3[d]	25	29.1	57.8	59.2	52.1	136.9	130.8	127.3	127.2	132.1	143.1
	−40	29.2	57.8	58.9	51.4	136.5	130.7	127.3	127.2	132.1	142.7
4[e]	25	31.1	58.4	59.8	56.8	137.9	131.5	127.7	127.7	132.7	144.0
	−93	28.9	56.8	58.6	54.2	136.6	130.9	127.7	127.7	131.9	143.1
5[f]	25	31.4	57.9	60.2	57.4	137.8	131.7	129.4	129.3	140.1	144.2
	−92	28.9	56.8	58.6	54.2	136.8	130.4	128.7	128.6	140.0	143.5
6[g]	25	31.1	58.7	59.7	56.5	138.4	131.3	127.8	127.8	132.9	143.8
	−93	29.9	57.9	58.9	55.2	137.7	131.0	127.4	127.4	132.4	143.2
7[h]	25	30.1	58.2	59.5	47.0	137.6	131.2	129.2	128.5	132.9	143.7
8[i]	25	32.2	57.2	58.5	67.1	136.4	130.7	127.6	127.4	132.3	142.3
9[j]	25	31.9	45.1	58.6	60.1	137.8	131.3	128.0	127.9	132.8	143.3
	−93	30.3	43.3	57.6	58.7	136.6	130.8	127.3	127.2	132.0	142.4
10[k]	25	30.8	60.2	61.1	47.9	137.9	131.9	128.0	127.9	132.9	143.1
	−93	29.4	59.3	62.1	45.5	137.0	131.7	127.6	127.5	132.5	142.1

Additional signals (δ/ppm and *J*/Hz): [a] Positions numbering is given in Schemes 2 and 4. [b] —; [c] CH_3-13.1 at 25 °C, CH_3 −12.3 at −93 °C; [d] C-5′-27.0, C-6′-29.5, C-7′-22.6, CH_3-14.1 at 25 °C, C-5′- 26.9, C-6′ −29.2, C-7′-22.6, CH_3 −14.1 at −40 °C; [e] ^{i}C-131.4, ^{o}C-130.4, ^{m}C-114.1, CH_3O-55.7 at 25 °C, ^{i}C-130.0, ^{o}C-129.8, ^{m}C-112.9, CH_3O-54.9 at −93 °C; [f] ^{i}C-130.4, ^{o}C-127.0, ^{m}C-114.1, CH_3-22.3; 55.7 (CH_3O) at 25 °C, ^{i}C-129.7, ^{o}C-126.4, ^{m}C-112.9, CH_3-22.2, 54.9 (CH_3O) at −92 °C; [g] ^{i}C-137.8, ^{o}C-128.8, ^{m}C-128.5, ^{p}C-130.7 at 25 °C, ^{i}C-137.1, ^{o}C-128.4, ^{m}C-130.3, ^{p}C-132.2 37.5 (C-5′), at −93 °C; [h] ^{i}C-137.7; ^{o}C-128.0, ^{m}C-128.5, ^{p}C-133.6, CO-199.1 at 25 °C; [i] ^{i}C-145.3, ^{o}C-119.1, ^{m}C-123.8, $^{m'}$C-127.2, $^{o'}$C-110.3, $^{i'}$C-132.5 (*Benzotriazol*-1-*yl*) at 25 °C; [j] ^{i}C-123.6, ^{o}C-132.1, ^{m}C-128.8, ^{p}C-123.6 at 25 °C, ^{i}C-122.2, ^{o}C-131.2, ^{m}C-128.1, ^{p}C-122.2, 86.5 (*C*≡C-CH_2), 85.1 (*C*≡C-CH_2) at 25 °C, 85.0 (*C*≡C-CH_2), 83.8 (C≡*C*-CH_2) at −93 °C; [k] 62.6 (d, *J* 6.8, O*C*H_2CH_3) at 25 °C, 60.6 (d, *J* 6.8, O*C*H_2CH_3) at −93 °C; 60.2 (d, *J* 9.0, O*C*H_2CH_3); 47.9 (d, *J* 167.8, *C*H_2P).

^{13}C NMR chemical shifts assignments of 1–10

The ^{13}C NMR spectra of **2**–**10** in CD_2Cl_2 solution are unchanged in the temperature range +25 °C to −93 °C (see Table 3), which confirms that there is only chair to chair exchange between mirror-image conformers. The spectral assignments of carbon signals are based on 2D HETCOR and HETCOR-LR and are reported in Table 3. At +25 °C to −93 °C, the ^{13}C NMR spectra of **2**–**10** (see Table 2) show signals for C-4′ of the *N*-alkyl group in the range of 44–48 ppm for compounds **1**, **2**, **7**, and **10** and in the range of 51–67 ppm for compounds **3**, **4**, **5**, **6**, **8** and **9**.

As a representative example of the HETCOR-LR spectra of **1**–**10** we have illustrated by arrows in Scheme 4 the typical long-range correlations through two or three bonds (J = 10 Hz) in **6**. The long-range shift correlation HETCOR-LR experiment, which was optimized at 10 Hz, was used to unambiguously distinguish two quaternary carbons (C-5a and C-9a).

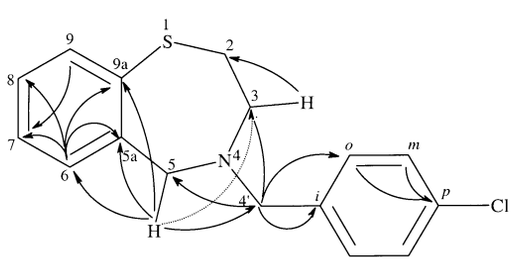

Scheme 4 Arrows represent typical C–H long range correlations through three bonds (J = 10 Hz) observed in the HETCOR-LR.

As a representative example of the low temperature two-dimensional ^{13}C–^{1}H correlated NMR spectra of **1**–**10**, we have included the contour plot (Fig. 5) of compound **2**, in which a cross peak was observed between a geminal pair of H-2 (2.40/2.89 ppm) and C-2/28 ppm, H-3 (3.18/3.39 ppm) and C-3/57.3 ppm, and between H-5 (3.94/4.25 ppm) and C-5/57.8 ppm.

Experimental

The ^{1}H and ^{13}C NMR spectra were acquired on a Varian GEMINI 300 spectrometer. Data were obtained from solution

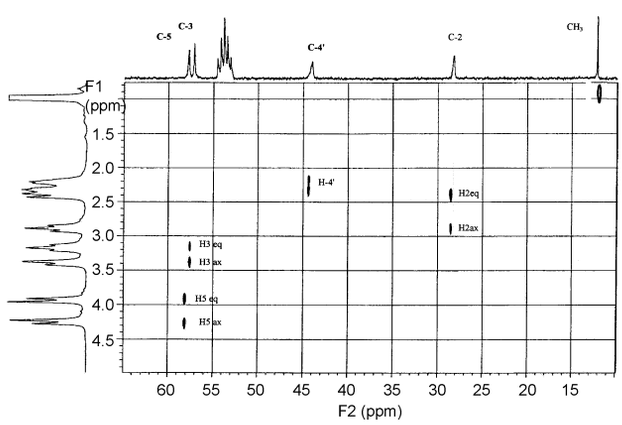

Fig. 5 HETCOR spectrum of **2** in CD_2Cl_2 (−93 °C).

in CD_2Cl_2 and the ^{1}H and ^{13}C NMR chemical shifts (δ) in ppm are referenced to the solvent peaks at 5.32 and 54.0 ppm, respectively. All two-dimensional experiments were acquired using standard Varian software. ^{11}B NMR spectrum were acquired on a VXR-300 MHz spectrometer operating at an observation frequency for ^{11}B (I = 3/2) of 96.2 MHz. The chemical shift scale was referenced to external $BF_3{\cdot}O(C_2H_5)_2$. The temperature was calibrated using a methanol and ethylene glycol standard for low and high temperatures, respectively. The temperature was accurate to ±0.5 °C. Compounds **1**–**10** were synthesized by known procedures.[4]

X-Ray crystallography

Data were collected with a Siemens SMART CCD area detector, using graphite monochromatized Mo-Kα radiation (λ = 0.71073 Å). The structure was solved by direct methods using SHELXS[16] and refined on F^2, using all data, by full-matrix least-squares procedures using SHELXL.[17] Hydrogen atoms were included in calculated positions, with isotropic displacement parameters 1.2 times the isotropic equivalent of their carrier atoms.

Crystal data for **1**: $C_{10}H_{16}BNS$, MW 193.11, triclinic, *P*-1, a = 7.128(2), b = 9.196(3), c = 9.506(3) Å, α = 62.984(3), β = 87.519(4), γ = 75.878(4) °, V = 536.7(3) Å^3, Z = 2, T = −105 °C,

$F(000) = 208$, $\mu(\text{MoK}\alpha) = 0.255\ \text{mm}^{-1}$, $D_{\text{calcd}} = 1.195\ \text{g.cm}^{-3}$, $2\theta_{\max}$ 50° (CCD area detector, 99% completeness), $wR(F^2) = 0.0908$ (all 1874 data), $R = 0.0328$ (1784 data with $I > 2\sigma I$).

References

1 (*a*) J. Szabó, G. Bernáth, Á. Katócs, L. Fodor and P. Sohár, *Can. J. Chem.*, 1987, **65**, 175; (*b*) A. K. Bose, W. A. Hoffman III and M. S. Manhas, *J. Chem. Soc., Perkin Trans. 1*, 1976, 2343; (*c*) L. H. Sternbach, H. Lehr, E. Reeder, T. Hayes and N. Steiger, *J. Org. Chem.*, 1965, **30**, 2812; (*d*) A. Garofalo, G. Campiani, S. M. Ciani, I. Fiorini and V. Nacci, *Tetrahedron*, 1996, **52**, 7745; (*e*) L. Fodor, J. Szabó, G. Bernáth and P. Sohár, *Tetrahedron Lett.*, 1995, **36**, 753; (*f*) M. Sindler-Kulyk, D. C. Neckers and J. R. Blount, *Tetrahedron*, 1981, **37**, 3377.

2 (*a*) M. Hachida, H. Lu, N. Kaneko, Y. Horikawa, A. Ohkado, H. Gu, X.-L. Zhang, H. Hoshi, M. Nonoyama, T. Nakanishi and H. Koyanagi, *Transplant. Proc.*, 1999, **31**, 996; (*b*) X. Yang, L. Buzon, E. Hamanaka and K. K.-C. Liu, *Tetrahedron: Asymmetry*, 2000, **11**, 4447; (*c*) D. H. G. Smith, J. M. Neutel and M. A. Weber, *Am. J. Hypertension*, 1999, **12**, 1030.

3 (*a*) R. B. English, P. T. Kaye, M. J. Mphahlele and R. D. Whittal, *J. Chem. Res. (S)*, 1995, 388 (*J. Chem. Res. (M)*, 1995, 2319); (*b*) Y. Ishihara, T. Tanaka, S. Miwatashi, A. Fujishima and G. Goto, *J. Chem. Soc., Perkin Trans. 1*, 1994, 2993.

4 A. R. Katritzky, Yong-Jiang Xu and Hai-Ying He, *J. Chem. Soc., Perkin Trans. 1*, 2002, 592.

5 (*a*) S. Désilets and M. St-Jacques, *J. Am. Chem. Soc.*, 1987, **109**, 1641; (*b*) R. St-Amour, M. T. P. Viet and M. St-Jacques, *Can. J. Chem.*, 1984, **62**, 2830; (*c*) A. Lachapelle and M. St-Jacques, *Can. J. Chem.*, 1987, **65**, 2575; (*d*) F. Sauriol-Lord and M. St-Jacques, *Can. J. Chem.*, 1979, **57**, 3221; (*e*) K. Von. Bredow, H. Friebolin and S. Kabuβ, *Org. Magn. Reson.*, 1970, **2**, 43; (*f*) H. Duddeck, M. Kaiser and A. Lévai, *Liebigs Ann. Chem.*, 1985, 869; (*g*) R. Glaser and B. Sklarz, *J. Chem. Soc., Perkin Trans. 2*, 1989, 1031; (*h*) P. W. W. Hunter and G. A. Webb, *Tetrahedron*, 1973, **29**, 147; (*i*) L. Sarrazin, M. Bourdeaux-Pontier, C. Briand and J. Vincent, *Org. Magn. Reson.*, 1975, **7**, 89; (*j*) D. Duval, P. Hennig, J. P. Bouchet, J. Vian, J. L. Peglion, J. P. Volland, N. Platzer and J. Guilhem, *Magn. Reson. Chem.*, 1997, **35**, 175; (*k*) A. Hassner and B. Amit, *Tetrahedron Lett.*, 1977, 3023.

6 F. G. Riddel, *The Conformational Analysis of Heterocyclic Compounds*, Academic Press, London, 1980, p. 22.

7 M. St-Jacques and C. Vaziri, *Org. Magn. Reson.*, 1972, **4**, 77.

8 (*a*) A. Flores-Parra, N. Farfán, A. I. Hernández-Bautista, L. Fernández-Sánchez and R. Contreras, *Tetrahedron*, 1991, **47**, 6903; (*b*) A. Flores-Parra, G. Cadenas-Pliego, L. M. R. Martínez-Aguilera, M. L. García-Nares and R. Contreras, *Chem. Ber.*, 1993, **126**, 863; (*c*) M. Güizado-Rodríguez, A. Flores-Parra, S. A. Sánchez-Ruiz, R. Tapia-Benavides, R. Contreras and V. I. Bakhmutov, *Inorg. Chem.*, 2001, **40**, 3243.

9 A. S. Batsanov, J. A. K. Howard, D. O'Hagan and M. Tavasli, *Acta Crystallogr., Sect. C: Cryst. Struct. Commun.*, 2000, **56**, E512.

10 H. Günther, *NMR Spectroscopy: Basic Principles, Concepts, and Applications in Chemistry*, Wiley & Sons Ltd, England, 2nd ed., 1995, p. 80.

11 P. Sóhar, *Nuclear Magnetic Resonance Spectrsocopy*, CRC Press, Roca Raton, Florida, 1983, vol. 2, p. 25.

12 C. Piccinni-Leopardi, O. Fabre and J. Reisse, *Org. Magn. Reson.*, 1976, **8**, 233.

13 R. Knorr, C. Ganter and J. D. Roberts, *Angew. Chem., Int. Ed. Engl.*, 1967, **6**, 556.

14 S. Von Kabuβ, H. Friebolin and H. Schmid, *Tetrahedron Lett.*, 1965, 469.

15 A. Mannschreck, G. Rissmann, F. Vögtle and D. Wild, *Chem. Ber.*, 1967, **100**, 335.

16 G. M. Sheldrick, *Acta Crystallogr., Sect. A*, 1990, **46**, 467.

17 G. M. Sheldrick, SHELXTL, Bruker Analytical X-ray Systems, 1997, Madison.